Subbarrier fusion in the interacting boson model

A. B. Balantekin, J. R. Bennett, and A. J. DeWeerd
Physics Department, University of Wisconsin, Madison, Wisconsin 53706

S. Kuyucak
Department of Theoretical Physics, Research School of Physical Sciences, Australian National University, GPO Box 4, Canberra, ACT 2601, Australia
(Received 2 July 1992)

A method is given for calculating the heavy ion subbarrier fusion cross section for nuclei which are described by the interacting boson model. Explicit formulas are given for the case when the target is rotational, including both quadrupole and hexadecapole couplings. Calculations of the fusion cross section, average angular momentum, and distribution of barriers for $^{16}O + ^{154}Sm$ are compared with experimental results and with predictions of the geometrical model.

PACS number(s): 25.70.Jj, 24.10.Eq, 21.60.Fw

I. INTRODUCTION

In this paper we study the effects of nuclear structure on heavy ion fusion near and below the Coulomb barrier. Many researchers have established that although a simple barrier penetration model of two colliding spherical nuclei describes well the fusion of light nuclei, this picture is insufficient to explain the magnitude of the fusion cross section for heavier nuclei at subbarrier energies [1]. Various studies [2–6] have argued that extra degrees of freedom such as static deformation [2], zero-point vibration [3], particle transfer [4], or neck formation [5] effectively lower the barrier and so enhance the cross section below the barrier. All of these mechanisms have previously been studied using the geometrical model of Bohr and Mottelson [7] and numerically solving coupled Schrödinger equations to take into account the different nuclear structure effects. In our work, we choose to study subbarrier fusion using instead the path integral formulation of the coupled-channels problem developed by Balantekin and Takigawa [8], taking into account the nuclear structure using the interacting boson model (IBM) [9]. This approach has the advantage of avoiding the complications of directly solving the Schrödinger equation for coupled channels. Also, the IBM can be applied to systems which are neither rotational nor vibrational, i.e., transitional nuclei between the SU(3) and SU(5) limits.

As many authors have shown [8, 10, 11], within the degenerate or "adiabatic" limit in which the excitation energies of the internal degrees of freedom can be neglected, the fusion probability can be written as a weighted sum over penetration probabilities through a set of one-dimensional barriers determined by diagonalization of the coupled-channels Hamiltonian. We derive an expression of this form for the cross section and then calculate the barrier transmission coefficients in a uniform WKB approximation to the path integral valid for energies both above and below the barrier [12, 13]. Throughout our calculation we use the notation of Ginocchio *et al.* [14, 15] and of Kuyucak and Morrison [16] to emphasize the similarity of our approach to their application of the IBM to proton scattering in the Glauber approximation.

Since several different mechanisms can account for the observed fusion cross sections for a given system, data on average angular momentum transfer provide a more stringent test of a model. In an earlier study [17], we outlined our method and compared our calculations with cross section and spin distribution data for ^{16}O on the deformed targets ^{154}Sm and ^{166}Er. Our previous work included only the effects of quadrupole collectivity by assuming that the target nuclei are described by the SU(3) limit of IBM. In this paper, we extend our formalism to allow multipoles of any order and present results including both quadrupole and hexadecapole couplings. Including the hexadecapole deformation increases the cross section and the angular momentum transfer at subbarrier energies, giving better agreement with the data than calculations including only quadrupole deformation.

Recently Rowley *et al.* [18] have suggested a method for determining the distribution of barriers in subbarrier fusion directly from the fusion cross section. Using their prescription we compare the barrier distribution obtained from our calculations with that obtained from precise cross section measurements carried out recently [19] for the system $^{16}O + ^{154}Sm$. We show directly the influences of quadrupole and hexadecapole couplings on the distribution of barriers.

In Sec. II of this paper we review our formalism which can be applied to any target describable by the IBM. We restrict our discussion to IBM-1, the version of IBM in which no distinction is made between neutrons and protons. We derive in Sec. III an expression for the fusion cross section for the case when the target or projectile is deformed. In Sec. IV we compare the results of numerical calculations with cross section, angular momentum, and distribution of barriers data for $^{16}O + ^{154}Sm$. Finally in Sec. V we discuss our approximations and conclusions.

II. APPLICATION OF IBM TO SUBBARRIER FUSION

We take the Hamiltonian for the system to be

$$H = -\frac{\hbar^2}{2\mu}\nabla^2 + V(r) + H_{\rm IBM} + H_{\rm int}, \tag{1}$$

where $\mathbf{r}$ is the relative coordinate of the target and projectile. The internuclear potential $V(r)$ is taken to be

$$V(r) = V_{\rm Coul}(r) + V_{\rm nuc}(r) \tag{2a}$$

where the nuclear part is

$$V_{\rm nuc}(r) = V_0\left(1 + e^{\frac{r-R_0}{a}}\right)^{-1}. \tag{2b}$$

This potential creates a barrier whose position, height, and curvature depend on the two charges and on the Woods-Saxon parameters V_0, R_0, and a, which will be specified later. $H_{\rm IBM}$ is the Hamiltonian describing the low-lying nuclear structure of the target (or projectile). When we make the adiabatic approximation the internal energies will be neglected and so the term $H_{\rm IBM}$ will be dropped. However, the IBM Hamiltonian is important as it distinguishes the various possible target structures in a way we will see later.

Finally, $H_{\rm int}$ represents the coupling to internal degrees of freedom. In the interacting boson model, the collective motions of an even-even nucleus are described by bosons representing correlated pairs of valence nucleons. In general, these bosons can carry any even angular momentum, although in practice it is found that only a few of the lowest angular momentum states need be included in order to describe a given nucleus. Introducing the boson operators $b_{\ell m}, \ell = 0, 2, 4, \ldots, \ell_{\rm max}$, we take $H_{\rm int}$ to be of the form of the most general one-body transition operator for IBM,

$$H_{\rm int} = \sum_{kj\ell} a_{kj\ell}(r)\left[b_j^\dagger \tilde{b}_\ell\right]^{(k)} \cdot Y^{(k)}(\hat{\mathbf{r}}). \tag{3}$$

The k sum runs over $k = 2, 4, \ldots, 2\ell_{\rm max}$. Odd values of k are excluded as a consequence of the reflection symmetry of the nuclear shape; the $k = 0$ term is already included in $V(r)$. For now we leave the form factors $\alpha_{kj\ell}(r)$ unspecified.

We would like to calculate the total fusion cross section using the barrier pentration picture in which it is assumed that once the projectile has tunnelled through the barrier it always fuses with the target. Hence it would be convenient to use the usual partial wave expansion

$$\sigma_{\rm fus}(E) = \pi\lambda\!\!\!^{-2}\sum_{\ell=0}^{\infty}(2\ell+1)T_\ell(E) \tag{4}$$

where T_ℓ are the penetration probabilities for the different partial waves. However, this expression is correct only under the approximation that the angular dependence of H can be ignored. Alternatively, we can perform a rotation at each instant to a frame in which the z axis points along the direction of relative motion. Neglecting the resulting centrifugal and Coriolis terms in the rotating frame is equivalent to ignoring the angular dependence of the original H. This same "rotating frame approximation" has been described by other authors [20–22] and has been shown [17, 20] to have the physical consequences that the coupling form factors become independent of ℓ and that only $m = 0$ magnetic substates of the target are excited. For heavy systems the neglected centrifugal and Coriolis forces are small. Hence we will first derive the transition probability within the rotating frame approximation. The result will be in general too unwieldy to give useful information, but we will see that in the semiclassical limit our formalism yields a simple result.

To simplify the calculation we first assume that the internal energies are small so that the term $H_{\rm IBM}$ can be neglected. We take the scattering to be in the x-y plane. Now making a rotation through the Euler angles [23] $\hat{\mathbf{b}} = (\phi, \pi/2, 0)$, we can write the Hamiltonian as the rotation of a simpler Hamiltonian depending only on the magnitude of $\mathbf{r}$

$$H = R(\hat{\mathbf{b}})H^{(0)}(r)R^\dagger(\hat{\mathbf{b}}). \tag{5}$$

$H_{\rm int}$ is the only term whose form is affected by the transformation. Hence we introduce the rotated interaction Hamiltonian $H_{\rm int}^{(0)}(r)$, given by

$$H_{\rm int} = R(\hat{\mathbf{b}})H_{\rm int}^{(0)}(r)R^\dagger(\hat{\mathbf{b}}), \tag{6a}$$

$$H_{\rm int}^{(0)}(r) = \sum_{j\ell m}\phi_{j\ell m}(r)b_{jm}^\dagger b_{\ell m}, \tag{6b}$$

$$\phi_{j\ell m}(r) = (-1)^m\sum_k\sqrt{\frac{2k+1}{4\pi}}\langle jm\ell - m|k0\rangle\alpha_{kj\ell}(r). \tag{6c}$$

Note that $H_{\rm int}^{(0)}$ is diagonal in the magnetic quantum number of the IBM state. Next, we introduce the evolution operator $\hat{U}$ for the system, which we write in terms of a reduced operator $\hat{U}^{(0)}$

$$\hat{U} = R(\hat{\mathbf{b}})\hat{U}^{(0)}. \tag{7}$$

Since $\hat{U}$ obeys the evolution equation

$$i\hbar\frac{\partial\hat{U}}{\partial t} = H\hat{U} \tag{8a}$$

subject to the initial condition

$$\hat{U}(t=0) = 1, \tag{8b}$$

we find using Eqs. (5), (7), and (8) that $\hat{U}^{(0)}$ satisfies the differential equation

$$i\hbar\frac{\partial\hat{U}^{(0)}}{\partial t} = \left[H^{(0)} - i\hbar R^\dagger(\hat{\mathbf{b}})\frac{\partial R(\hat{\mathbf{b}})}{\partial t}\right]\hat{U}^{(0)}, \tag{9a}$$

$$\hat{U}^{(0)}(t=0) = 1. \tag{9b}$$

Now making the rotating frame approximation, we drop the last term in Eq. (9a). As we will see, the transition probability can be expressed in terms of $\hat{U}^{(0)}$ so that the time-dependent rotation angle $\hat{\mathbf{b}}$ does not appear. In this approximation, we can apply a partial wave expansion in the orbital angular momentum. We will first calculate the transmission probability for the $\ell = 0$ partial wave.

Then in the spirit of the rotating frame approximation we assume that the only angular momentum dependence of the transmission probability for the higher partial waves comes from the centrifugal potential, and we take the coupling form factors to be independent of ℓ.

Now we have simplified the problem to the calculation of the transition amplitude for each partial wave. It is convenient to formulate this problem using path integral techniques [8] since then we can make use of the extensive work already done on semiclassical approximation to path integrals. Consider then a barrier in one dimension, corresponding to the Coulomb, nuclear, and centrifugal potentials for a given partial wave. In addition, the interaction energy represented by $H_{\rm int}^{(0)}$ raises or lowers this barrier slightly, depending on the internal state of the target. The propagator to go from an initial state characterized by relative radial coordinate (the magnitude of r) r_i and IBM quantum numbers n_i to a final state r_f and n_f may be written [11]

$$K(r_f,n_f,T;r_i,n_i,0)=\int\mathcal{D}\left[r(t)\right]e^{\frac{i}{\hbar}S(r,T)}W_{n_fn_i}(r(t),T), \tag{10}$$

where $S(r,T)$ is the action for the translational motion and $W_{n_fn_i}$ is the propagator for the internal system:

$$W_{n_fn_i}(r,T)=\left\langle n_f\left|R(\hat{\mathbf{b}})\hat{U}_{\rm int}^{(0)}(r(t),T)\right|n_i\right\rangle. \tag{11}$$

$\hat{U}_{\rm int}^{(0)}$ satisfies the differential equation

$$i\hbar\frac{\partial\hat{U}_{\rm int}^{(0)}}{\partial T}=H_{\rm int}^{(0)}\hat{U}_{\rm int}^{(0)}, \tag{12a}$$

$$\hat{U}_{\rm int}^{(0)}(t=0)=1. \tag{12b}$$

We want to consider the case where r_i and r_f are on opposite sides of the barrier. In the limit when the initial and final states are far away from the barrier, the transition amplitude is given by the S-matrix element, which can be expressed in terms of the propagator [8]

$$S_{n_f,n_i}(E)=-\frac{1}{i\hbar}\lim_{\substack{r_i\to\infty\\ r_f\to-\infty}}\left(\frac{p_ip_f}{\mu^2}\right)^{\frac{1}{2}}\exp\left[\frac{i}{\hbar}(p_fr_f-p_ir_i)\right]\times\int_0^\infty dTe^{+iET/\hbar}K(r_f,n_f,T;r_i,n_i,0), \tag{13}$$

where p_i and p_f are the classical momenta associated with r_i and r_f. In heavy ion fusion we are interested in the transition probability in which the internal system emerges in any final state. This is

$$T_\ell=\sum_{n_f}|S_{n_f,n_i}(E)|^2, \tag{14a}$$

which becomes, upon substituting Eqs. (10) and (13),

$$T_\ell=\lim_{\substack{r_i\to\infty\\ r_f\to-\infty}}\left(\frac{k_ik_f}{\mu^2}\right)\int_0^\infty dTe^{\frac{i}{\hbar}ET}\int_0^\infty\widetilde{T}e^{-\frac{i}{\hbar}E\widetilde{T}}\int\mathcal{D}[r(t)]\int\mathcal{D}[\tilde{r}(\tilde{t})]\exp^{\frac{i}{\hbar}[S(r,T)-S(\tilde{r},\widetilde{T})]}\rho_M(\tilde{r}(\tilde{t}),\widetilde{T};r(t),T). \tag{14b}$$

Here we have again assumed that the energy dissipated to the internal system is small compared to the total energy and taken p_f outside the sum over final states. We identified the two-time influence functional as

$$\rho_M(\tilde{r}(\tilde{t}),\widetilde{T};r(t)T)=\sum_{n_f}W_{n_f,n_i}^*(\tilde{r}(\tilde{t});\widetilde{T},0)W_{n_f,n_i}(r(t);T,0). \tag{14c}$$

Using the completeness of final states one sees that the two-time influence functional simplifies to become the matrix element of a unitary operator in the initial state of the internal system:

$$\rho_M=\left\langle n_i\left|\hat{U}_{\rm int}^{0\dagger}(\tilde{r},\widetilde{T})\hat{U}_{\rm int}^{0}(r,T)\right|n_i\right\rangle. \tag{15}$$

The interaction Hamiltonian was chosen to be a linear combination of boson operators. From a group theoretical point of view, these operators form an SU(n) algebra, where $n=\frac{1}{2}\ell_{\max}(\ell_{\max}+3)+1$. Hence the operator $\hat{U}^{(0)}$ is an element of the group SU(n). The boson states form a basis for the symmetric irreducible representation of SU(n) of rank N, where N is the number of bosons in the target. If we assume now that the form factors $\alpha_{kj\ell}(r)$ are all proportional to the same function of r then the Hamiltonian $H_{\rm int}^{(0)}$ commutes with itself at different times and hence we can write

$$\rho_M=\left\langle n_i\left|e^{\frac{i}{\hbar}\int_0^{\widetilde{T}}dtH_{\rm int}^{(0)}(\tilde{r}(t))}e^{-\frac{i}{\hbar}\int_0^{T}dtH_{\rm int}^{(0)}(r(t))}\right|n_i\right\rangle. \tag{16}$$

Furthermore, the exponents of the two operators in the influence functional commute and hence ρ_M becomes the matrix element of an SU(n) transformation between SU(n) basis states, in other words it is a representation matrix element for the group. Now it is straightforward to calculate the necessary matrix element. We will calculate the matrix element in the next section for the case when the target is a rotational nucleus. Here we give the rest of the procedure for calculating the fusion cross section, assuming that the matrix element has been calculated.

Barrier penetration in the path integral formalism has been considered previously by Brink and Smilansky [12, 13].

They derived a simple formula for the transmission probability using a uniform semiclassical approximation to the path integral, valid for energies both above and below the barrier. Their essential conclusion is that the penetration probability, expressed as

$$P(E) = \lim_{\substack{r_i\to\infty \\ r_f\to-\infty}} \left(\frac{k_i k_f}{\mu^2}\right) \int_0^\infty dT e^{\frac{i}{\hbar}ET} \int_0^\infty d\tilde{T} e^{-\frac{i}{\hbar}E\tilde{T}} \int \mathcal{D}[r(t)] \int \mathcal{D}[\tilde{r}(\tilde{t})] e^{\frac{i}{\hbar}[S(r,T)-S(\tilde{r},\tilde{T})]}, \tag{17}$$

can be evaluated to give

$$P(E) = \left(1+e^{2Q}\right)^{-1}, \tag{18a}$$

$$Q = \sqrt{\frac{2\mu}{\hbar^2}} \int_{r_1}^{r_2} dr[V(r)-E]^{\frac{1}{2}}. \tag{18b}$$

This is the familiar WKB result, and r_1 and r_2 are the classical turning points of the motion. Our expression (14b) for T_ℓ is nearly the same as the one they derive, except that they do not consider coupling to internal degrees of freedom and hence in their case the two-time influence functional reduces simply to unity. We can nevertheless use their result, provided that we express the two-time influence functional as an exponential or sum of exponentials, for then the exponents can be combined with the actions of the path integrals and regarded as effective potentials. The transmission coefficients can then be evaluated numerically simply by solving the WKB integral in Eq. (18b). Hence, using Eqs. (17) and (18) in Eq. (14b), and inserting this into Eq. (4), our formula for the cross section takes the form

$$\sigma_{\text{fus}}(E) = \pi\lambda\!\!\!^{-2} \sum_{\ell=0}^{\infty} (2\ell+1) \sum_i \omega_i T_\ell \left(E - V_{\text{eff}}^{(i)}\right), \tag{19}$$

where the ω_i are the appropriate weight factors and the effective potentials are a sum of the Coulomb, nuclear, and centrifugal potentials, plus perturbations due to the influence functional which are linear combinations of the form factors $\alpha_{kj\ell}(r)$. The transmission coefficients are to be evaluated using the WKB expressions Eqs. (19).

III. CALCULATION OF THE INFLUENCE FUNCTIONAL

The needed matrix element has been calculated by Kuyucak and Morrison [16] and for limiting cases by Ginocchio *et al.* [14]. The matrix element depends on the details of the IBM state of the target and hence on the choice of IBM Hamiltonian. It is convenient here to use the fact that the IBM state can be projected out from an intrinsic state [24, 25]. Thus for the ground state band one can express the intrinsic state of the target as

$$|\phi_g\rangle = \frac{1}{\sqrt{N!}} (b^\dagger)^N |0\rangle \tag{20a}$$

where we introduced an intrinsic boson operator for a rotational nucleus given by,

$$b^\dagger = \sum_\ell x_\ell b_{\ell 0}^\dagger. \tag{20b}$$

The intrinsic state depends on the IBM Hamiltonian by way of the mean field amplitudes x_0 and x_2. In practice one must first choose a Hamiltonian which describes well the low-lying levels of the target nucleus. Then the mean field amplitudes can be gotten by minimizing the energy in a variational calculation, for example.

The general result for the matrix element is rather complicated, so here we give only the formula for the case when $\ell_{\max} = 2$ (s-d boson model). Then the only possible transition operators that can be formed are $(b_0^\dagger \tilde{b}_{2m} + b_{2m}^\dagger b_0)$, $[b_2^\dagger \tilde{b}_2]_m^{(2)}$, and $[b_2^\dagger \tilde{b}_2]_m^{(4)}$. For the first operator we have taken the Hermitian combination of b_0 and b_2 which yields real matrix elements. We again note the assumption that all the form factors $\alpha_{kj\ell}(r)$ are proportional to the same function of r. We denote this function by $g(r)$ and take

$$\begin{aligned} &\alpha_{202}(r) = \alpha_{220}(r) = g(r), \\ &\alpha_{222}(r) = x g(r), \\ &\alpha_{422}(r) = y g(r). \end{aligned} \tag{21}$$

The constants x and y and the function $g(r)$ will be specified later. We assume that the initial state of the target is the ground state. Denoting the number of bosons in the target by N, one finds that the matrix element can be written [16]

$$\rho_M = \int \sin\theta d\theta d\phi \sin\theta' d\theta' d\phi' f^N, \tag{22a}$$

where f is a polynomial in trigonometric functions of θ, θ', ϕ, and ϕ' with coefficients which are exponentials of the form factors. We can write

$$\begin{aligned} f = {} & 4Ae^{i\hat{g}(10x+3y)} \sin^2\theta \sin^2\theta' \cos^2(\phi-\phi') - 2Ae^{i\hat{g}(10x+3y)} \sin^2\theta \sin^2\theta' \\ & + 8Ae^{-i\hat{g}(5x+12y)} \sin\theta\cos\theta\sin\theta'\cos\theta'\cos(\phi-\phi') + Be^{i\hat{g}(-5x+9y+\eta)} \\ & + Ce^{i\hat{g}(-5x+9y+\eta)} \cos^2\theta + Ce^{i\hat{g}(-5x+9y+\eta)} \cos^2\theta' + De^{i\hat{g}(-5x+9y+\eta)} \cos^2\theta\cos^2\theta' \\ & + Ee^{i\hat{g}(-5x+9y-\eta)} + Fe^{i\hat{g}(-5x+9y-\eta)} \cos^2\theta + Fe^{i\hat{g}(-5x+9y-\eta)} \cos^2\theta' + Ge^{i\hat{g}(-5x+9y-\eta)} \cos^2\theta\cos^2\theta', \end{aligned} \tag{22b}$$

where we defined

$$\hat{g}(r) = \frac{1}{\sqrt{280\pi}} g(r), \tag{22c}$$

$$\eta = 5\sqrt{14 + x^2 + \frac{81}{25}y^2 - \frac{18}{5}xy}, \tag{22d}$$

and the coefficients are

$$\begin{aligned}
A &= \frac{3}{8}x_2^2, \\
B &= x_0^2\frac{\eta + 5x - 9y}{2\eta} - x_0x_2\frac{5\sqrt{14}}{2\eta} + x_2^2\frac{\eta - 5x + 9y}{8\eta}, \\
C &= x_0x_2\frac{15\sqrt{14}}{4\eta} - 3x_2^2\frac{\eta - 5x + 9y}{8\eta}, \\
D &= 9x_2^2\frac{\eta - 5x + 9y}{8\eta}, \\
E &= x_0^2\frac{\eta - 5x + 9y}{2\eta} + x_0x_2\frac{5\sqrt{14}}{2\eta} + x_2^2\frac{\eta + 5x - 9y}{8\eta}, \\
F &= -x_0x_2\frac{15\sqrt{14}}{4\eta} - 3x_2^2\frac{\eta + 5x - 9y}{8\eta}, \\
G &= 9x_2^2\frac{\eta + 5x - 9y}{8\eta}.
\end{aligned} \tag{22e}$$

We can simplify the matrix element by expanding f^N in a multinomial series and integrating the trigonometric functions term by term. Note that one of the integrals over either ϕ or ϕ' is trivial and gives just 2π. Since the integrands are simply powers of $\sin\theta$ and other standard functions, the other integrals can be carried out using standard tables. We then obtain a linear combination of exponentials, each of which provides an effective potential depending on the constants x and y and the function $g(r)$. Then inserting the matrix element in Eq. (14), combining the effective potentials with the actions and using the semiclassical approximation to the path integrals described in the previous section, we are finally faced only with the numerical evaluation of the WKB integral Eq. (18b) for each partial wave.

IV. RESULTS OF NUMERICAL CALCULATIONS

We have used Eq. (19) to consider the fusion of ^{16}O with ^{154}Sm. The Coulomb barrier for this system is around 59.2 MeV, as determined from recent fusion data at energies above the barrier [19]. The samarium nucleus is highly deformed and hence one supposes the coupling in this case could excite the low-lying rotational 2^+ and perhaps 4^+ states at 82 and 267 keV for a projectile with center-of-mass energy near or below the Coulomb barrier. For the internal Hamiltonian we used an extension [26] of the "consistent-Q" parametrization of Warner and Casten [27],

$$H_{\rm IBM} = \epsilon n_d + \kappa Q^2 + \kappa' L^2, \tag{23a}$$

where n_d is the d-boson number operator, Q is the quadrupole operator, and L is the angular momentum operator of the IBM:

$$n_d = \sum_m b_{2m}^\dagger b_{2m}, \tag{23b}$$

$$Q_m = b_0^\dagger \tilde{b}_{2m} + b_{2m}^\dagger b_0 + \chi\left[b_2^\dagger \tilde{b}_2\right]_m^{(2)}, \tag{23c}$$

$$L_m = \sqrt{10}\left[b_2^\dagger \tilde{b}_2\right]_m^{(1)}. \tag{23d}$$

We found $\epsilon = 550$ keV, $\kappa = -24$ keV, $\kappa' = -3.5$ keV, and $\chi = -1.15$ to give an accurate representation of the low-lying structure of ^{154}Sm. Note that we work in the s-d boson model. The mean fields were then calculated using a code developed by Kuyucak [28] which minimizes the energy in a variational calculation; we find $x_0 = 0.742$ and $x_2 = 0.670$.

We expect the matrix elements of the transition operators to scale with the number of bosons N in the target, so in order to make the average interaction energy independent of N we choose the form factor $g(r)$ to scale inversely as the matrix element of the quadrupole transition operator. Hence we introduce the reduced form factor $f(r)$,

$$g(r) = \frac{f(r)}{\langle 2_1^+ \parallel Q \parallel 0_1^+\rangle}. \tag{24}$$

The reduced quadrupole matrix element has been calculated as an expansion in powers of $1/N$ (N is the number of bosons) and is given by [29]

$$\langle 2_1^+ \parallel Q \parallel 0_1^+\rangle = N\left(2x_0x_2 - \sqrt{\tfrac{2}{7}}\chi x_2^2\right). \tag{25}$$

We take the reduced form factor to be proportional to the quadrupole fields of the deformed target:

$$f(r) = f_{\rm Coul}(r) + f_{\rm nuc}(r), \tag{26a}$$

where the Coulomb part is [2]

$$f_{\rm Coul}(r) = \frac{3}{\sqrt{20\pi}}\beta Z_1 Z_2 e^2 \frac{R_c^2}{r^3} (r > R_c) \tag{26b}$$

$$= \frac{3}{\sqrt{20\pi}}\beta Z_1 Z_2 e^2 \frac{r^2}{R_c^3} (r > R_c) \tag{26c}$$

and the nuclear part is [11]

$$f_{\rm nuc}(r) = -\sqrt{\frac{5}{4\pi}}\beta R_V \frac{dV_{\rm nuc}}{dr}. \tag{26d}$$

In our calculations we take $R_c = 1.2A^{\frac{1}{3}}$ fm and $R_c = 1.2A^{\frac{1}{3}}$ fm, where A is the mass number of the deformed target. β is a parameter which measures the strength of the coupling between the translational motion and the internal states of the target.

For the Woods-Saxon parameters we chose values which give a Coulomb barrier with a height of 58.3 MeV, slightly less than that determined from the data. We found $V_0 = 130.0$ MeV, $R_0 = 7.5$ fm, and $a = 1.2$ fm to give a satisfactory barrier. The remaining free parameters in our calculations were then the coupling strengths β, x, and y. However, in the consistent-Q formalism one takes the parameter x in the quadrupole transition op-

erator to be the same as the χ in the IBM Hamiltonian. Hence we have already determined x to be -1.15, leaving two free parameters, the overall coupling strength β, and the hexadecapole strength y. In addition, we studied the behavior of our results when the number of bosons in the target was varied. For ^{154}Sm, the actual number of bosons is $N = 11$ and hence the maximum angular momentum of the target state is 22 in our model which includes only s ($\ell = 0$) and d ($\ell = 2$) bosons. However, by setting $N = 1$ for example, we can study a hypothetical Sm nucleus in which there is only a single excited 2^+ state in addition to the ground state, and thus by changing N we can see the importance of including the different higher states in the ground state rotational band.

In Fig. 1 we compare results of our calculations to recent data on the ^{16}O + ^{154}Sm fusion cross section taken by Wei *et al.* [19]. The position of the barrier with no coupling is indicated by the arrow. One sees that the calculated cross section (solid curve) agrees with the data quite well. For this calculation we found the couplings $\beta = 0.328$, $y = 2.15$ to give the best fit. In our previous work, which included only quadrupole coupling, we noted that the effect of the quadrupole coupling is to increase the cross section dramatically for energies below the barrier. As we will demonstrate below, the effect of the hexadecapole coupling is to increase the cross section below the barrier somewhat more.

The dotted curve represents the fusion cross section calculated when all couplings are set equal to zero, or equivalently when the number of bosons in the target is set equal to zero. One sees there the huge effect which the couplings have on the subbarrier fusion cross section. Finally, the dashed curve shows the fusion cross section calculated when the target boson number is set equal to four. Here one observes the well known effect that the cross section rapidly "saturates" as more channels are added in a coupled-channels calculation, and there is little difference between the calculations for $N = 4$ and for higher numbers of bosons. In our previous work [17] we showed how the cross section and angular momentum remained unchanged when the number of bosons in the target nucleus was increased beyond 1 or 2. In our current calculations, we see that these quantities saturate as the number of bosons reaches 4 or 5. It takes at least 2 bosons in the s-d IBM in order for the target to have an excited 4^+ state. Hence the hexadecapole coupling is only effective for N at least 2, and so we expect the saturation to take place at a somewhat larger number of bosons in our present calculations.

In Fig. 2 we show the average angular momentum as a function of energy calculated using the same potential and couplings as were used for the cross section. One sees that the calculation using the IBM (solid curve) gives good agreement with the data for energies near and above the barrier but is too small for subbarrier energies. This missing angular momentum could be a signal that g bosons play an important role in the coupling of ^{154}Sm to the fusion channel. In our study we included hexadecapole couplings through an $\ell = 4$ term in the transition operator, but we did not include any additional hexadecapole coupling arising from the presence of g bosons. The large bump in the curve has been observed before and has a simple explanation in terms of the barrier penetration picture [32].

For comparison we show with the dashed curve the average angular momentum calculated using the coupled-channels code CCDEF [33], including quadrupole, octupole and hexadecapole couplings [31]. The better agreement of the coupled-channels calculation than the IBM calculation with the data may be due to our neglect of the octupole vibration state and of g bosons. The dotted curve shows the predicted average angular momentum for a spherical potential (all couplings set equal to zero).

As Rowley *et al.* [18] have pointed out, the distribution of barriers in subbarrier fusion can be gotten from the

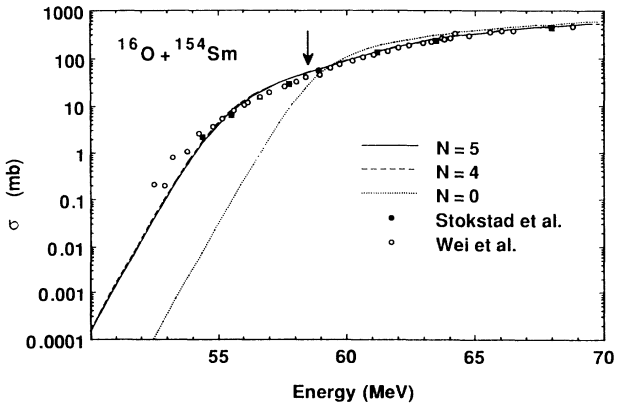

FIG. 1. Comparison of predicted cross section using the interacting boson model with experimental data from Wei *et al.* [19] (open circles) and Stokstad [30] (dark circles). The different curves correspond to including different numbers of bosons in the calculation: $N = 5$ (solid curve), $N = 4$ (dashed curve), and $N = 0$ (dotted curve).

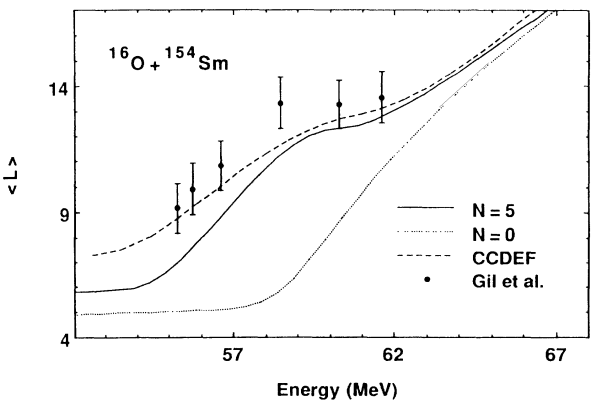

FIG. 2. Comparison of predicted average angular momentum using the interacting boson model (solid curve) with that using the geometrical model (dashed curve) and with the case of a spherical potential and no coupling (dotted curve). Experimental data from Gil *et al.* [31].

fusion cross section by considering the quantity

$$\frac{d^2}{dE^2}\left[E\sigma(E)\right].$$

To calculate the second derivative requires accurate knowledge of the cross section for many closely spaced energies. The measurements of Wei *et al.* [19] allow such a determination to be made and in Fig. 3 we compare the predictions of the IBM calculation (solid curve) to their measurements of the barrier distribution. Again the potential and couplings are the same as for the calculations in Figs. 1 and 2. The width of the distribution is about 10 MeV, and the maximum occurs near the energy of the barrier (indicated by the arrow in Fig. 1). Evidently the couplings can raise or lower the barrier by several MeV. In calculating the distribution of barriers we used the simple approximation

$$\frac{d^2}{dE^2}f(E) \approx \frac{f(E+\delta E) - 2f(E) + f(E-\delta E)}{\delta E^2}, \qquad (27)$$

where δE is some suitable small energy interval. We chose $\delta E = 2$ MeV, corresponding to the value used by Wei *et al.* [19] in reporting their data.

To understand better the effects of the various couplings in our calculations, we examined the cross section, angular momentum, and barrier distribution as the couplings were varied. In Figs. 4, 5, and 6 we show how changing the magnitude of the hexadecapole coupling y while keeping the quadrupole couplings fixed affects the calculations. In Figs. 4 and 5, we see that both the cross section and the angular momentum increase below the barrier with increasing y; the behavior is opposite slightly above the barrier, and the calculations remain unchanged well above the barrier. Previous studies [34] have noted that the magnitude of the subbarrier cross section enhancement can be quite different depending on the sign of the hexadecapole coupling. Arguments have been made to show that either positive or negative hexadecapole moments are more effective at increasing the cross section [34]. Figure 4 indicates that positive hexadecapole coupling gives a larger subbarrier fusion cross section by about a factor of 2 for the case of ^{16}O+ ^{154}Sm.

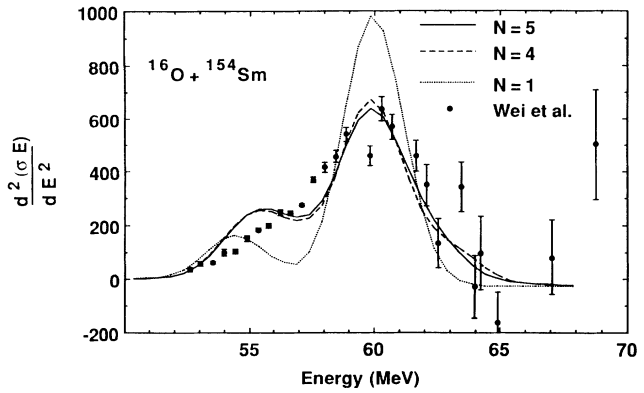

FIG. 3. Comparison of predicted distribution of barriers using the interacting boson model (solid curve) with experimental data from Wei *et al.* [19].

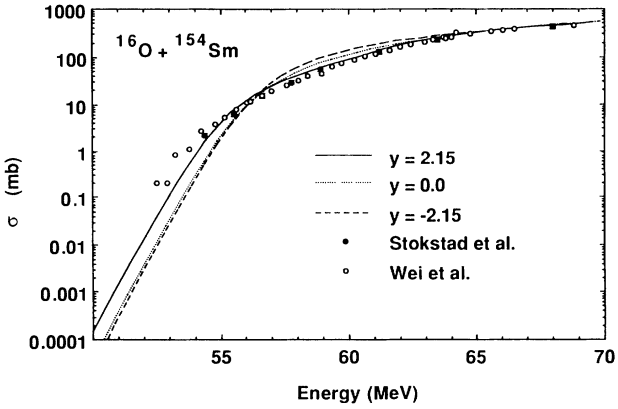

FIG. 4. The effect of changing hexadecapole coupling y on cross section is shown. Solid curve is $y = 2.15$, dotted curve $y = 0.0$, and dashed curve $y = -2.15$. The quadrupole coupling is fixed ($x = -1.15$, $\beta = 0.328$).

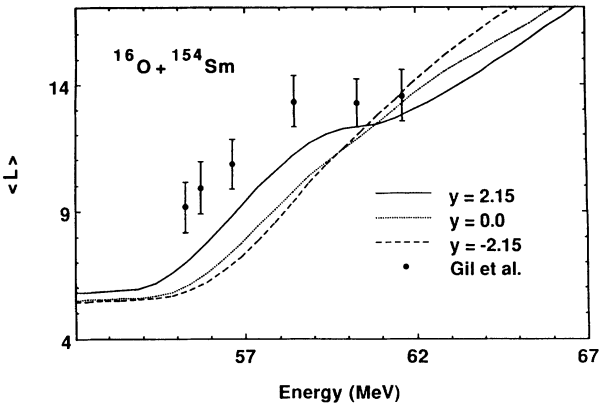

FIG. 5. Effect of changing hexadecapole coupling on average angular momentum for fixed quadrupole coupling ($x = -1.15, \beta = 0.328$). Solid curve is $y = 2.15$, dotted curve $y = 0.0$, and dashed curve $y = -2.15$.

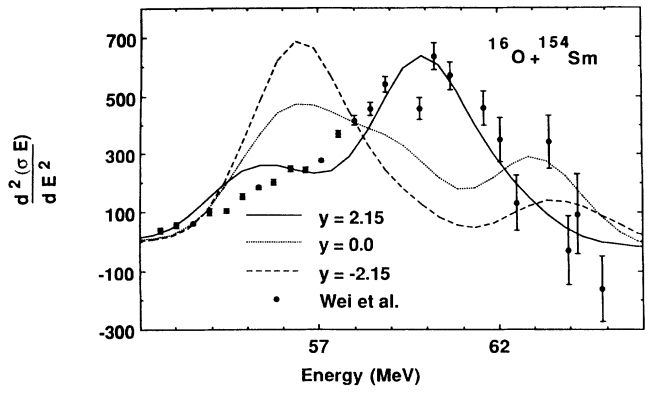

FIG. 6. Effect of changing hexadecapole coupling on distribution of barriers for fixed quadrupole coupling (all parameters same as in Figs. 4 and 5).

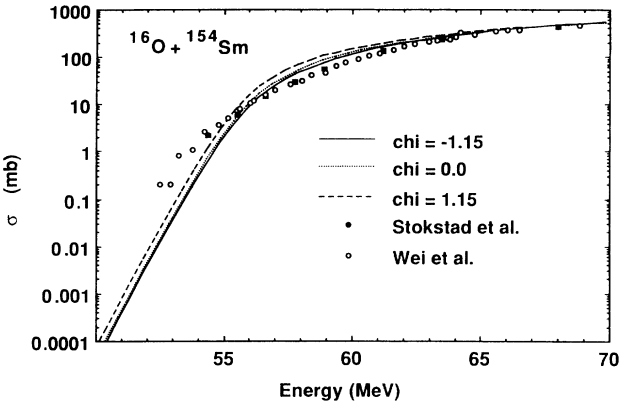

FIG. 7. Effect of changing quadrupole coupling on fusion cross section for zero hexadecapole coupling ($y = 0.0$). Solid curve for $x = -1.15$, dotted curve for $x = 0.0$, and dashed curve for $x = 1.15$. In all cases, $\beta = 0.328$.

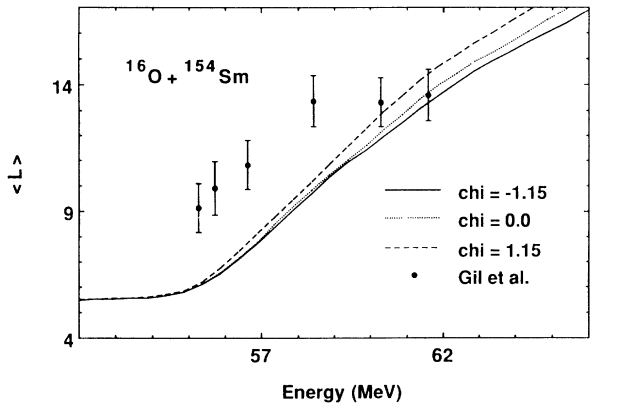

FIG. 8. Effect of changing quadrupole coupling on average angular momentum for zero hexadecapole coupling ($y = 0.0$). The quadrupole parameters are the same as in Fig. 7.

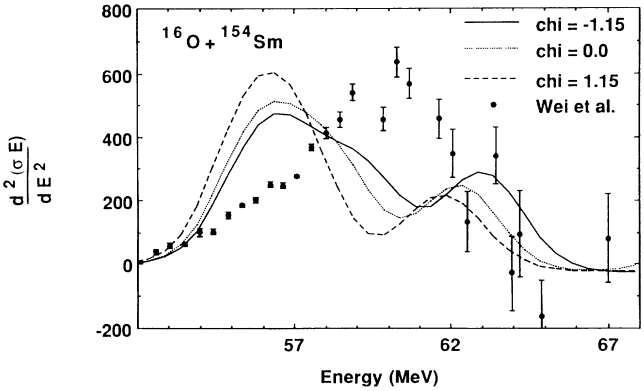

FIG. 9. Effect of changing quadrupole coupling on distribution of barriers for zero hexadecapole coupling ($y = 0.0$). Quadrupole parameters are the same as in Figs. 7 and 8.

The main point, however, is that adding a positive hexadecapole coupling improves the agreement of the calculation with the cross section and angular momentum data.

In Fig. 6 we see how the hexadecapole coupling can dramatically affect the distribution of barriers. The distribution is skewed to higher or lower energies depending on whether the coupling is positive or negative. Thus examination of the fusion barrier distribution gives directly the sign of the hexadecapole coupling.

In Figs. 7, 8, and 9 we study the effect of changing the parameter χ. In the IBM, $\chi > 0$ indicates oblate deformation, $\chi < 0$ prolate, and $\chi = 0$ the gamma-unstable limit. Although ^{154}Sm is prolate, it is nevertheless interesting to see how the calculations change as one goes from one limit to another.

V. CONCLUSIONS

Our calculations using the interacting boson model agree reasonably well with data on the subbarrier fusion of ^{16}O with ^{154}Sm. This is not surprising since the IBM is known to describe well the collective properties of heavy ions. From these studies one would like to be able to draw conclusions about the physical processes which take place during heavy ion fusion. However as Krappe *et al.* [5] have pointed out, even though a model for subbarrier fusion predicts correctly the experimental data it is not easy to identify the underlying physical mechanisms which are being modelled. This ambiguity arises because essentially any coupling introduced between the translational motion and other degrees of freedom will increase the subbarrier fusion cross section.

In our study it would seem that the couplings introduced are modelling several things. Firstly, the spatial dependence of the form factors was chosen to correspond to the quadrupole Coulomb and nuclear fields of a deformed nucleus. As is well known, the potential barrier depends on the orientation of the deformed target and by including more rotational states in a coupled-channels analysis one is essentially performing a weighted average of the cross section over a distribution of barriers corresponding to the different orientations [35]. Hence in our study we include the effect of the different orientations through the form chosen for the coupling functions. The different effective potentials all contain a coupling proportional to the same radial function, with various weights corresponding to the different orientations of the deformed nucleus. The couplings were also chosen to be proportional to the most general $E2$ and $E4$ transition operator in the s-d boson model. This choice represents the assumption that the couplings can induce such transitions. The parameter y then represents the relative importance of hexadecapole to quadrupole transitions, x represents the relative importance of seniority-conserving to seniority-breaking quadrupole transitions, and β is an overall multiplicative factor which represents both the amount of target deformation and the strength of the transition operator. Note that the way in which we include hexadecapole transitions, through the term $[d^\dagger \tilde{d}]^{(4)}$ in the interaction Hamiltonian, accounts only for part of

the $E4$ transitions. To fully model these transitions requires introducing g bosons. This representation of the hexadecapole transitions may be the reason for the seemingly large value of y we have found to fit the data best.

From these considerations we might conclude that the enhanced subbarrier fusion cross section is due to the ability of the projectile to exploit the lower barriers for certain target orientations and to the presence of extra channels corresponding to the target's low-lying excited states. The agreement of this model with the angular momentum and barrier distribution data gives further confidence that this is the case. According to a study of Pacheco *et al.* [36], neutron transfer does not seem to be the mechanism responsible for the subbarrier fusion enhancement of $^{16}O + {}^{154}Sm$, although it may well play a role in other systems.

The interacting boson model and geometrical model give equivalent results for the subbarrier fusion cross section in the case of the rather "clean" system we have studied, where the target is well deformed and the projectile spherical and basically structureless in the context of low-energy fusion. In this case it seems arguable that the fusion enhancement is due to the deformation of the target and to excitation of its low-lying rotational states. Surely, though, the fusion process is more complex than our simple barrier penetration picture even for this case, and for more complicated systems the competing channels such as transfer and dynamical neck formation may be important in determining the outcome of the collision. To describe such a situation seems a formidable task. One advantage of the IBM approach is that it avoids the numerical complications of solving coupled differential equations for the different channels. In addition, although both the IBM and the geometrical model can describe well the low-energy properties of rotational and vibrational nuclei, the IBM can also successfully describe many properties of transitional nuclei which do not fall into one of these limiting cases and for which a geometrical picture in terms of shape variables is somewhat difficult to implement. Especially in these cases the IBM may provide a convenient way to describe nuclear structure effects in subbarrier fusion.

ACKNOWLEDGMENTS

We thank R. Vandenbosch for useful discussions. This research was supported in part by the U.S. National Science Foundation Grant No. PHY-9015255. The research of A.B.B. was further supported in part by a Presidential Young Investigator Program administered by the U.S. National Science Foundation. The research of S.K. was supported in part by the Australian Research Council.

[1] M. Beckerman, Rep. Prog. Phys. **51**, 1047 (1988).
[2] R.G. Stokstad and E.E. Gross, Phys. Rev. C **23**, 281 (1981).
[3] H. Esbensen, Nucl. Phys. **A352**, 147 (1981).
[4] R.A. Broglia, C.H. Dasso, S. Landowne, and A. Winther, Phys. Rev. C **27**, 2433 (1983).
[5] H.J. Krappe, K. Mohring, M.C. Nemes, and H. Rossner, Z. Phys. A **314**, 23 (1983).
[6] C.H. Dasso, S. Landowne, and A. Winther, Nucl. Phys. **A405**, 381 (1983).
[7] A. Bohr and B. Mottelson, K. Dan. Vidensk. Selsk. Mat. Fys. Medd. **27**, 16 (1953).
[8] A.B. Balantekin and N. Takigawa, Ann. Phys. (N.Y.) **160**, 441 (1985).
[9] F. Iachello and A. Arima, *The Interacting Boson Model* (Cambridge University Press, Cambridge, England, 1987).
[10] P.M. Jacobs and U. Smilansky, Phys. Lett. **127B**, 313 (1983).
[11] R. Lindsay and N. Rowley, J. Phys. G **10**, 805 (1984).
[12] D.M. Brink and U. Smilansky, Nucl. Phys. **A405**, 301 (1983).
[13] D.M. Brink, *Semi-classical Methods for Nucleus-Nucleus Scattering* (Cambridge University Press, Cambridge, England, 1985).
[14] J.N. Ginocchio, T. Otsuka, R.D. Amado, and D.A. Sparrow, Phys. Rev. C **33**, 247 (1986).
[15] J.N. Ginocchio, Nucl. Phys. **A421**, 369c (1984).
[16] S. Kuyucak and I. Morrison (unpublished).
[17] A.B. Balantekin, J.R. Bennett, and N. Takigawa, Phys. Rev. C **44**, 145 (1991).
[18] N. Rowley, G.R. Satchler, and P.H. Stelson, Phys. Lett. B **254**, 25 (1991).
[19] J.X. Wei, J.R. Leigh, D.J. Hinde, J.O. Newton, R.C. Lemmon, S. Elfstrom, J.X. Chen, and N. Rowley, Phys. Rev. Lett. **67**, 3368 (1991).
[20] O. Tanimura, Phys. Rev. C **35**, 1600 (1987).
[21] H. Esbensen, S. Landowne, and C. Price, Phys. Rev. C **36**, 1216 (1987).
[22] N. Takigawa and K. Ikeda, in *Proceedings of the Symposium on Many Facets of Heavy Ion Fusion Reactions*, edited by W. Hennings *et al.*, Argonne National Laboratory Report ANL-PHY-87-1, 1986, pp. 613–620.
[23] M.E. Rose, *Elementary Theory of Angular Momentum* (Wiley, New York, 1957).
[24] J.N. Ginocchio and M.W. Kirson, Nucl. Phys. **A350**, 31 (1980).
[25] A.E.L. Dieperink, O. Scholten, and F. Iachello, Phys. Rev. Lett. **44**, 1747 (1980).
[26] P.O. Lipas, P. Toivonen, and D.D. Warner, Phys. Lett. **155B**, 295 (1985).
[27] D.D. Warner and R.F. Casten, Phys. Rev. Lett. **48**, 1385 (1982); Phys. Rev. C **28**, 1798 (1983).
[28] S. Kuyucak (unpublished).
[29] S. Kuyucak and I. Morrison, Ann. Phys. (N.Y.) **181**, 79 (1988).
[30] R.G. Stokstad *et al.*, Phys. Rev. C **21**, 2427 (1980).
[31] S. Gil, R. Vandenbosch, A. Charlop, A. Garcia, D.D. Leach, S.J. Luke, and S. Kailas, Phys. Rev. C **43**, 701 (1991).
[32] S. Gil *et al.*, Phys. Rev. Lett. **65**, 3100 (1990).
[33] J. Fernandez Niello, C.H. Dasso, and S. Landowne, Comput. Phys. Commun. **54**, 409 (1989).
[34] M.J. Rhoades-Brown and V.E. Oberacker, Phys. Lett. **50**, 1435 (1983); M.J. Rhoades-Brown *et al.*, Z. Phys. A **310**, 287 (1983).
[35] M.A. Nagarajan, A.B. Balantekin, and N. Takigawa, Phys. Rev. C **34**, 894 (1986).
[36] A.J. Pacheco *et al.*, Z. Phys. A **331**, 451 (1988).